Communication

Observations on the Nonlinear Unloading Behavior of Advanced High Strength Steels

ERIK J. PAVLINA, MYOUNG-GYU LEE, and FRÉDÉRIC BARLAT

The unloading behavior was compared for three different steel grades: a dual-phase steel, a transformation-induced plasticity steel, and a twinning-induced plasticity steel. Steels that harden by phase transformation or deformation twinning exhibited a smaller component of microplastic strain during unloading and a smaller reduction in the chord modulus compared to the conventional hardening steel. As a result, unloading is closer to pure elastic unloading when the TRIP effect or TWIP effect is active.

DOI: 10.1007/s11661-014-2688-0

When steels are deformed in uniaxial tension and then unloaded, the total recovered strain is greater than what is predicted by linear (and nonlinear) elasticity theory.[1–18] The total unloading strain comprises an elastic component, a thermal component related to adiabatic heating, and an additional strain component that has been attributed to dislocation relaxation phenomena or nonhomogeneous deformation in the case of multiphase steels.[5,6,9,17] As a result of this additional component of the unloading strain, the relationship between stress and strain is nonlinear during unloading. Increased deformation (or higher stress in the material) prior to unloading results in greater deviations from linear unloading behavior.

If dislocation relaxation phenomena are responsible for this additional strain component on unloading, then the additional strain can be called as a microplastic strain.[8,16] Recently, Kim *et al.*[16] suggested that the microplastic component of the unloading strain is proportional to the amount of strain hardening (*i.e.*, increase in flow strength) prior to unloading. They proposed that the microplastic component of the unloading strain, ε_{mp}, can be given by

$$\varepsilon_{mp} = \frac{K}{M\alpha\mu\sqrt{1-K}}(\sigma - \sigma_0), \qquad [1]$$

where σ is the flow strength at the start of unloading, σ_0 is the yield strength, M is the Taylor factor, α is an empirical factor, μ is the shear modulus, and K is a constant less than 1 and relates the mobile dislocation density to the total dislocation density. Equation [1] assumes that the total amount of strain hardening is the result of the increase of dislocation density with strain and the increased probability of dislocation interactions with defects and other barriers to dislocation motion and that hardening follows the Kocks–Mecking hardening rule for polycrystals.[19] However, in many advanced high strength steels (AHSS), strain hardening may also occur *via* phase transformation as in the case of transformation-induced plasticity (TRIP) steels or *via* deformation twinning as in the case of twinning induced plasticity (TWIP) steels.[20–22] As a result, if these other strain hardening mechanisms are active then the increase in flow strength after yielding (*i.e.*, $\sigma - \sigma_0$) can be simply expressed as

$$\sigma - \sigma_0 = \Delta\sigma_{dislocation} + \Delta\sigma_{TRIP} + \Delta\sigma_{TWIP}, \qquad [2]$$

where $\Delta\sigma_{dislocation}$, $\Delta\sigma_{TRIP}$, and $\Delta\sigma_{TWIP}$ represent the increase in flow strength due to dislocation interactions, the TRIP effect, and the TWIP effect, respectively. In Eq. [2], $\Delta\sigma_{dislocation}$ takes the form of the classic Taylor equation (*i.e.*, $\Delta\sigma_{dislocation} = M\alpha\mu\sqrt{\rho}$), and $\Delta\sigma_{TRIP}$ and $\Delta\sigma_{TWIP}$ are related to the fraction of austenite transformed to martensite or the deformation twin fraction, respectively, and can be considered a type of dynamic dispersion strengthening or composite strengthening effect.[20–22] Transformation and twinning kinetics are controlled by the chemical composition, the temperature and strain rate of deformation, the crystallographic texture, and the deformation mode.[23,24]

Equation [1] assumes that that all of the strain hardening is attributed to dislocation interactions (*i.e.*, $\sigma - \sigma_0 = \Delta\sigma_{dislocation}$ and $\Delta\sigma_{TRIP} = \Delta\sigma_{TWIP} = 0$). If the nonlinear unloading behavior is the result of dislocation relaxation phenomena as proposed by others,[5,6] then it can be postulated that the microplastic component of the unloading strain should decrease when $\Delta\sigma_{TRIP}$ or $\Delta\sigma_{TWIP}$ are nonzero because $\Delta\sigma_{dislocation}$, which is related to the dislocation density, is a smaller fraction of the total increment of strain hardening $(\sigma - \sigma_0)$. This supposition is investigated by comparing the unloading behavior of three steels that strain harden *via* different basic mechanisms—a dual-phase (DP) steel, a TRIP steel, and a TWIP steel. The DP steel represents strain hardening by only dislocation interactions (*i.e.*, $\sigma - \sigma_0 = \Delta\sigma_{dislocation}$), the TRIP steel represents hardening by combined dislocation interactions and the TRIP effect (*i.e.*, $\sigma - \sigma_0 = \Delta\sigma_{dislocation} + \Delta\sigma_{TRIP}$), and the TWIP steel represents hardening by combined dislocation interactions and the TWIP effect (*i.e.*, $\sigma - \sigma_0 = \Delta\sigma_{dislocation} + \Delta\sigma_{TWIP}$). The application of Eq. [1] to TRIP or TWIP steels assumes no contribution

ERIK J. PAVLINA, Research Fellow, is with the Institute for Frontier Materials, Deakin University, 75 Pigdons Road, Waurn Ponds, VIC 3216, Australia. MYOUNG-GYU LEE, Associate Professor, is with the Department of Materials Science and Engineering, Korea University, Anam-dong, Seongbuk-gu, Seoul 136-701, Korea. Contact e-mail: myounglee@korea.ac.kr FRÉDÉRIC BARLAT, Professor and Director of Materials Mechanics Laboratory, is with the Graduate Institute for Ferrous Technology, Pohang University of Science and Technology, Pohang, Gyeongbuk 790-784, South Korea.

Manuscript submitted August 26, 2014.
Article published online December 3, 2014

of the TRIP or TWIP strain hardening mechanisms to the mobile dislocation density and it provides a means to compare and interpret the unloading behavior and springback of different AHSS grades. Detailed microstructural evaluation was outside the scope of the present work and this investigation provides the first comparison of the nonlinear unloading behavior of these three important steel grades.

Three different sheet steel grades were examined in this study: a Fe-0.07C-2.2Mn-1.0Si (in wt pct) dual-phase (DP) steel, a Fe-0.14C-2.0Mn-1.3Al TRIP steel, and a Fe-0.66C-17.5Mn-1.2Al TWIP steel (source: POSCO). Uniaxial tensile tests and uniaxial loading–unloading–loading tests were conducted using standard size ASTM E8[25] tensile specimens with a 50-mm gage length. All tests were performed under displacement control (nominal strain rate of 0.9×10^{-4} s^{-1}) and at room temperature. Strain was measured using an extensometer, and the initial elastic moduli were calculated by the impulse excitation of vibration method according to ASTM E1876.[26] In the uniaxial loading–unloading–loading tests, the forward and reverse crosshead/actuator displacement rates were equal in magnitude. The unloading behavior was compared after deforming the specimens between an engineering strain of 1 pct and just before the uniform elongation. Table I summarizes the engineering strain unloading (*i.e.*, pre-strain) used for the loading–unloading–loading tests for each of the steel grades. Two or three tests were conducted for each level of deformation. Comparisons between the different steel grades were made using the microplastic component of the unloading strain (ε_{mp}), the chord modulus on unloading (E_{chord}), and the dissipated energy represented by the hysteresis in the unloading–loading portion of the stress–strain curve. Figure 1 illustrates these three measures on a loading–unloading–loading test of the DP steel pre-strained to 7.5 pct and then unloaded and then reloaded. The start of the unloading curve was defined by the maximum strain reached in forward deformation prior to the start of unloading.

Figure 2 shows representative stress–strain curves of the three steel grades. Table II summarizes the mechanical properties of the DP steel, TRIP steel (initial austenite fraction of 9 pct), and TWIP steel. The uncertainty is given by the 95 pct confidence interval (CI) calculated from the tests. In the case of the TWIP steel, the uniform elongation exceeded the limits of the extensometer. All three steels exhibit similar, but not identical, yield strengths that range between 480 and 540 MPa.

Figure 3 compares the microplastic component of the unloading strain of the DP, TRIP, and TWIP steels after uniaxial tensile deformation. For a given increase in flow strength due to strain hardening (*i.e.*, larger value of $\sigma - \sigma_0$), the DP steel exhibits a greater microplastic component of unloading strain compared to the TRIP and TWIP steels. In effect, in steels which exhibit the TRIP or TWIP effect, the contribution of dislocation generation and increased dislocation interactions to the total amount of strain hardening is decreased (*i.e.*, the total dislocation density required to achieve the same amount of strengthening is smaller when either $\Delta\sigma_{TRIP}$ or $\Delta\sigma_{TWIP}$ is nonzero). As a result, the microplastic component of unloading strain is decreased for equal values of total strain hardening in the TRIP and TWIP steels compared to the DP steel.

Equation [1] indicates that the microplastic component of strain should be zero when the strain hardening increment, $\sigma - \sigma_0$, is zero but the linear regression of the data (dashed lines in Figure 3) suggests a nonzero intercept. The nonzero intercept may be attributed to

Table I. Engineering Strain at Unloading (Pre-strain) Used for Loading–Unloading–Loading Tests

Steel	Engineering Strain at Unloading (pct)
DP	1, 2.5, 5, 7.5, 10, 12
TRIP	1, 2.5, 5, 6.5, 7.5, 8.5, 10, 12, 14
TWIP	5, 25, 40

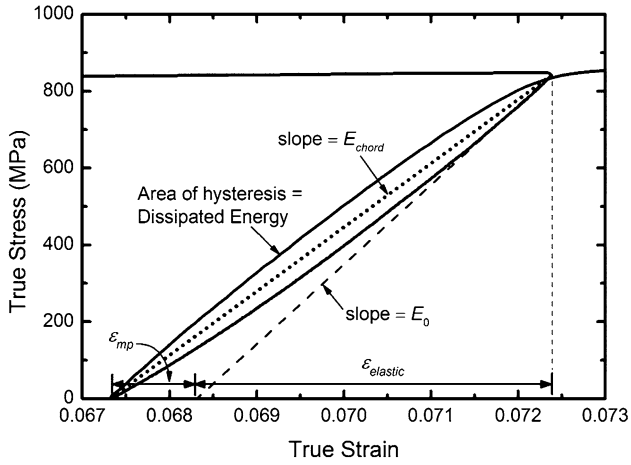

Fig. 1—Example of the stress–strain behavior during a loading–unloading–loading test of the DP steel deformed to an engineering strain of 7.5 pct, unloaded, and then reloaded. The microplastic component (ε_{mp}) of the unloading strain, the chord modulus (E_{chord}), and the hysteresis of the unloading–loading loop are indicated.

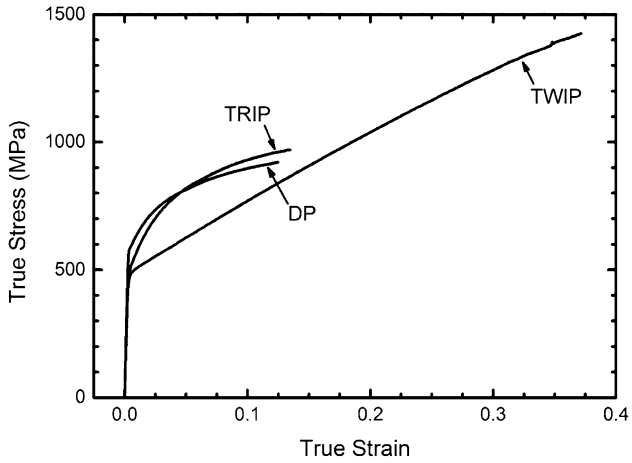

Fig. 2—Representative true stress-true strain curves for the DP, TRIP, and TWIP steels.

Table II. Mechanical Properties of DP, TRIP, and TWIP Steels

Steel	Yield Strength[a] (MPa)	Ultimate Tensile Strength (MPa)	Uniform Elongation (pct)	E_0 (GPa)	Thickness (mm)
DP	540 ± 2	814 ± 2	14.0 ± 0.1	207	1.75
TRIP	500 ± 5	851 ± 6	15.6 ± 0.2	200	1.20
TWIP	480 ± 3	>1000	>50	183	1.25

[a]0.2 pct offset method.

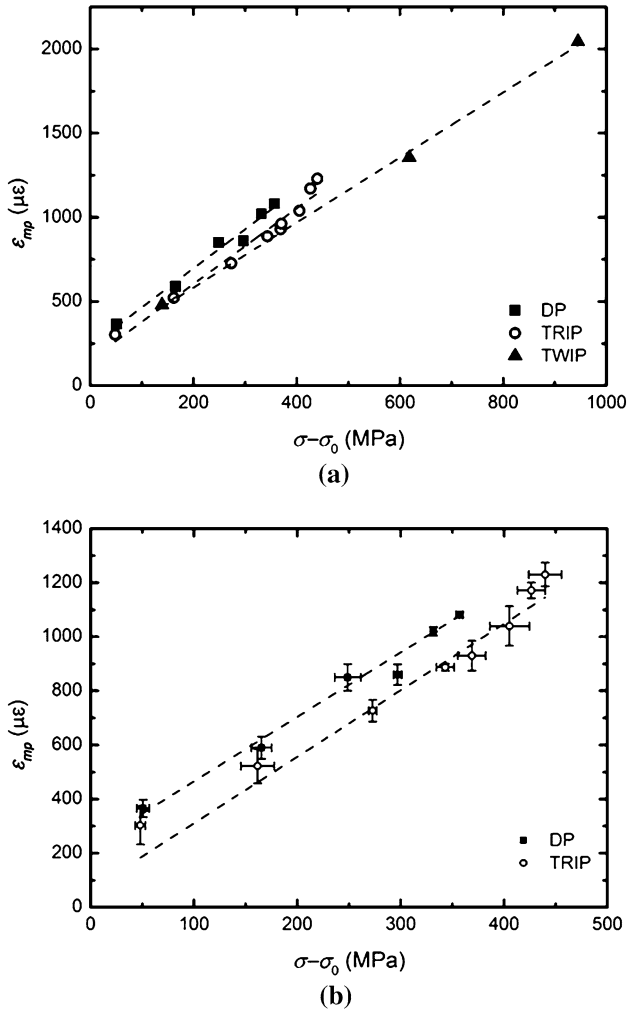

Fig. 3—Comparison of the microplastic component of the unloading strain following uniaxial tensile deformation for (*a*) the DP, TRIP, and TWIP steels and (*b*) expanded to only show the DP and TRIP steels. Uncertainty is ±95 pct CI.

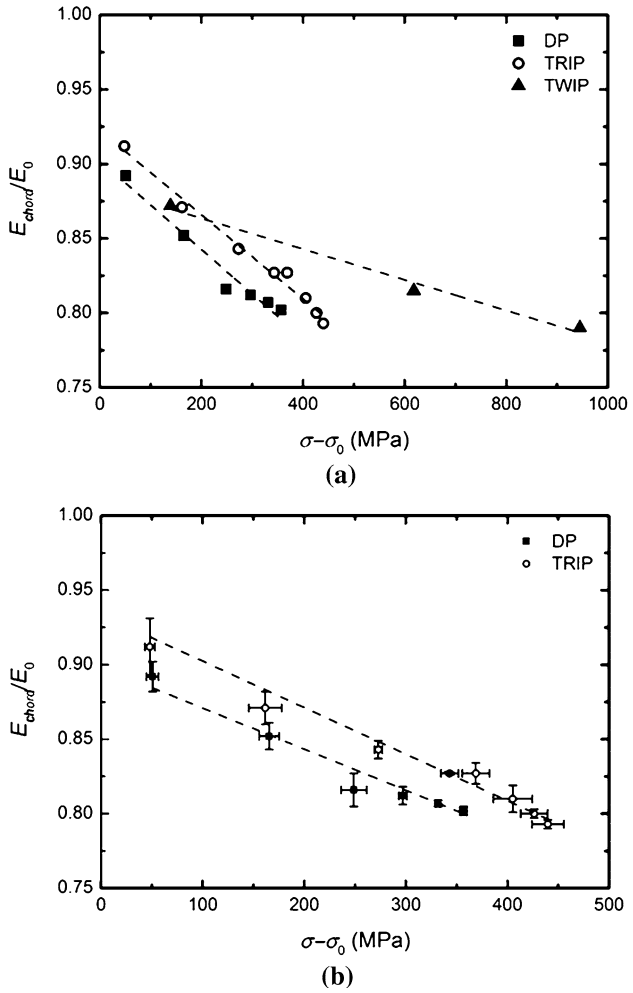

Fig. 4—Comparison of the reduction in the chord modulus after uniaxial tensile deformation for (*a*) the DP, TRIP, and TWIP steels and (*b*) expanded to only show the DP and TRIP steels. The dashed lines are for clarity only and are not intended to suggest any functional relationship for the data. Uncertainty is ±95 pct CI.

the use of the macroscopic yield strength for σ_0, which is measured after microyielding and deviations from linear elasticity have already occurred. As a result, some microplastic component of the unloading strain might be expected for $\sigma - \sigma_0 = 0$ and this behavior near the macroscopic yield strength strain should be investigated in the future.

Figure 4 compares the chord modulus of the DP, TRIP, and TWIP steels after tensile deformation. In Figure 4, the chord modulus is normalized to the initial elastic modulus and so a value of E_{chord}/E_0 equal to 1 would represent pure linear elastic unloading. Per unit of strain hardening, the chord modulus of the TRIP and TWIP steels decreases less than that of the DP steel. The reduction in the chord modulus of the TRIP and TWIP steels is smaller because the microplastic component of unloading strain represents a smaller fraction of the total unloading strain for the TRIP and TWIP steels compared to the DP steel (Figure 5).

Figure 6 compares the area of the hysteresis loop made by the unloading-loading stress–strain curve. The area of the hysteresis loop represents the dissipated

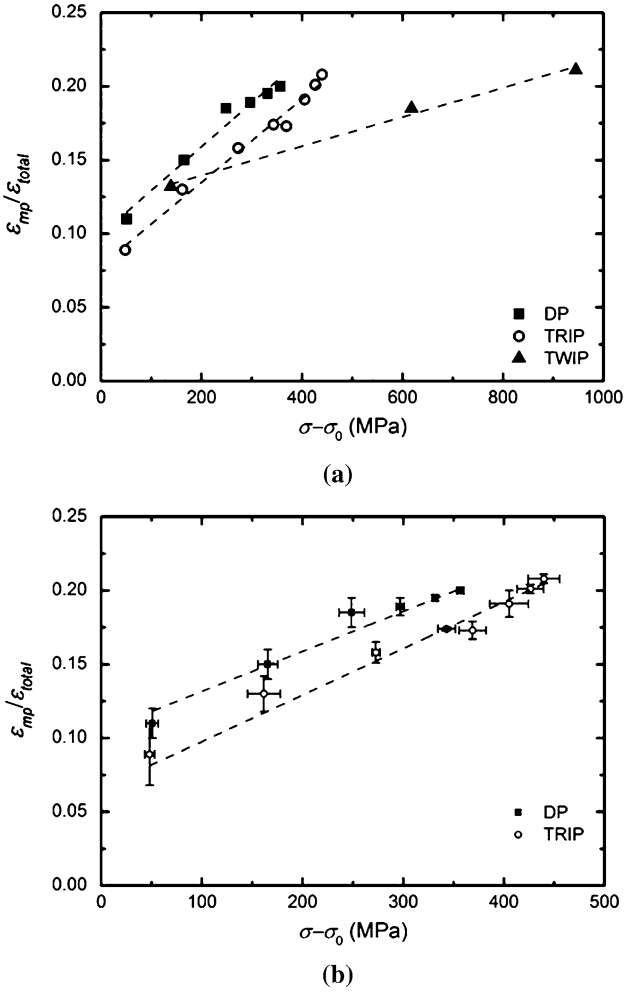

Fig. 5—Comparison of the contribution of the microplastic component of unloading strain to the total unloading strain for (*a*) the DP, TRIP, and TWIP steels deformed in uniaxial tension and then unloaded and (*b*) expanded to only show the DP and TRIP steels. The dashed lines are for clarity only and are not intended to suggest any functional relationship for the data. Uncertainty is ±95 pct CI.

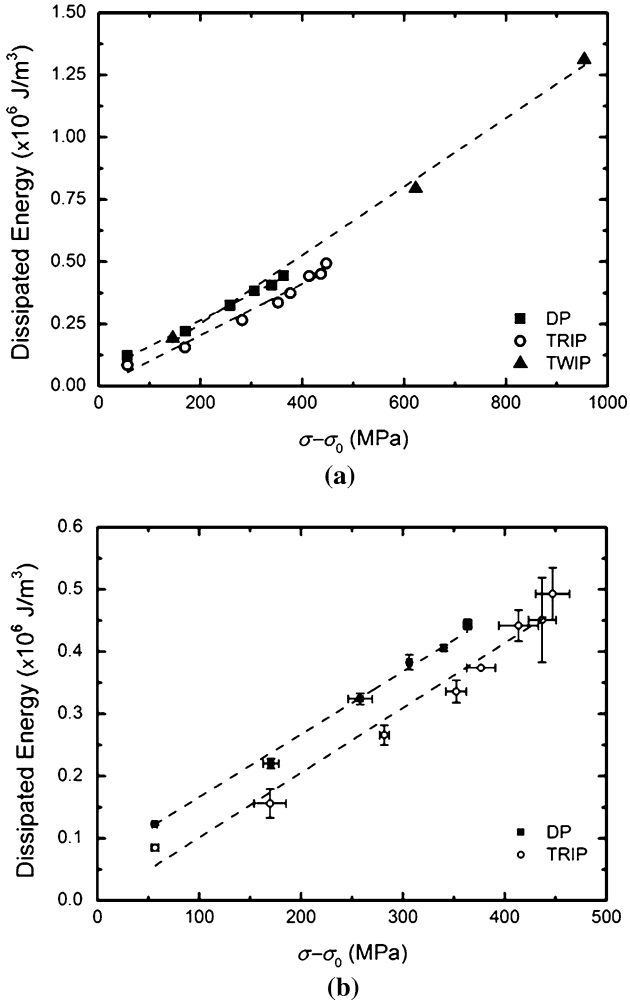

Fig. 6—Comparison of the dissipated energy during unloading and reloading following uniaxial tensile deformation for (*a*) the DP, TRIP, and TWIP steels and (*b*) expanded to only show the DP and TRIP steels. The dashed lines are for clarity only and are not intended to suggest any functional relationship for the data. Uncertainty is ±95 pct CI.

energy of the unloading-loading deformation process and it has been used to characterize the nonlinear nature of the unloading–loading behavior of AHSS.[15] Per increment of strain hardening, more energy is dissipated in the DP steel compared to the TRIP steel. However, the DP and TWIP steels exhibit similar amounts of dissipated energy per increment of strain hardening. The cause of this similar behavior is unknown, but it may be related to a detwinning mechanism in the TWIP steel during unloading and reloading and more investigation is necessary. Because the fraction of the microplastic component of unloading strain to the total unloading strain is smaller in the TRIP steel compared to the DP steel, the TRIP steel dissipates less energy during the unloading-loading deformation cycle. These results again show that when a steel hardens *via* the TRIP effect, features of the unloading curve related to the microplastic strain component and the nonlinearity are reduced compared to steels that harden only *via* dislocation generation and increased dislocation interactions.

In summary, these results indicate that the unloading behavior, or springback, of AHSS is affected by the active strain hardening mechanisms. The unloading behavior following uniaxial tensile deformation of steels that exhibit the TRIP effect or TWIP effect is closer to pure elastic unloading when compared to steels of comparable strength that harden only by conventional strain hardening means (*i.e.*, increased dislocation density and dislocation interactions). This investigation shows that the TRIP and TWIP effects are effective at reducing the microplastic component of unloading strain and minimizing the reduction in the chord modulus on unloading. These results indicate that it may be possible to modify the unloading behavior (and springback) of AHSS through careful control of the structure of the steel. In essence it may be possible to design a low springback AHSS grade. Such design requires more investigation of the effects of microstructural features (*e.g.*, grain size, phase fraction, phase hardness, *etc.*) on the unloading behavior and coupling

with appropriate strain hardening models before it is realized.

The authors would like to acknowledge POSCO for supplying the steel used in this investigation. M.-G. Lee appreciates support by the National Research Foundation of Korea (NRF) Grant funded by the Korea government (MSIP) (No. 2012R1A5A1048294) and industrial source technology development program (#10040078) of MKE.

REFERENCES

1. F. Morestin, M. Boivin, and C. Silva: *J. Mater. Process. Technol.*, 1996, vol. 56, pp. 619–30.
2. F. Morestin and M. Boivin: *Nucl. Eng. Des.*, 1996, vol. 162, pp. 107–16.
3. K. Yamaguchi, H. Adachi, and N. Takakura: *Met. Mater. Int.*, 1998, vol. 4, pp. 420–25.
4. F. Yoshida, T. Uemori, and K. Fujiwara: *Int. J. Plast*, 2002, vol. 18, pp. 633–59.
5. R.M. Cleveland and A.K. Ghosh: *Int. J. Plast*, 2002, vol. 18, pp. 769–85.
6. L. Luo and A.K. Ghosh: *J. Eng. Mater. Technol.-Trans. ASME*, 2003, vol. 125, pp. 237–46.
7. M. Yang, Y. Akiyama, and T. Sasaki: *J. Mater. Process. Technol.*, 2004, vol. 151, pp. 232–36.
8. R. Pérez, J.A. Benito, and J.M. Prado: *ISIJ Int.*, 2005, vol. 45, pp. 1925–33.
9. B.S. Levy, C.J. Van Tyne, Y.H. Moon, and C. Mikalsen: SAE Technical Paper 2006-01-0146, 2006.
10. D. Fei and P. Hodgson: *Nucl. Eng. Des.*, 2006, vol. 236, pp. 1847–51.
11. E.J. Pavlina, B.S. Levy, C.J. Van Tyne, S.O. Kwon, and Y.H. Moon: *Int. J. Mod. Phys. B*, 2008, vol. 22, pp. 6070–75.
12. P.A. Eggertsen and K. Mattiasson: *Int. J. Mech. Sci.*, 2009, vol. 51, pp. 547–63.
13. H.Y. Yu: *Mater. Des.*, 2009, vol. 30, pp. 846–50.
14. P.A. Eggertsen and K. Mattiasson: *Int. J. Mater. Form.*, 2010, vol. 3, pp. 127–30.
15. L. Sun and R.H. Wagoner: *Int. J. Plast.*, 2011, vol. 27, pp. 1126–44.
16. H. Kim, C. Kim, F. Barlat, E. Pavlina, and M.-G. Lee: *Mater. Sci. Eng. A*, 2013, vol. 562, pp. 161–71.
17. A. Govik, R. Rentmeester, and L. Nilsson: *Mater. Sci. Eng. A*, 2014, vol. 602, pp. 119–26.
18. Y.P. Korkolis, N. Deng, and T. Kuwabara: *Numisheet 2014 AIP Conference Proceedings*, AIP Publishing, 2013, vol. 1567, pp. 700–04.
19. H. Mecking and U.F. Kocks: *Acta Metall.*, 1981, vol. 29, pp. 1865–75.
20. P.J. Jacques, Q. Furnémont, F. Lani, T. Pardoen, and F. Delannay: *Acta Mater.*, 2007, vol. 55, pp. 3681–93.
21. O. Bouaziz, S. Allain, and C. Scott: *Scripta Mater.*, 2008, vol. 58, pp. 484–87.
22. J. Gil Sevillano: *Scripta Mater.*, 2009, vol. 60, pp. 336–39.
23. L. Samek, E. De Moor, J. Penning, and B.C. De Cooman: *Metall. Mater. Trans. A*, 2006, vol. 37A, pp. 109–24.
24. O. Bouaziz, S. Allain, C.P. Scott, P. Cugy, and D. Barbier: *Curr. Opin. Solid State Mater. Sci.*, 2011, vol. 15, pp. 141–68.
25. ASTM E8/8M-11, Annual Book of ASTM Standards, vol. 3.01. American Society for Testing and Materials, West Conshohocken, Pennsylvania.
26. ASTM E1876-09, Annual Book of ASTM Standards, vol. 3.01. American Society for Testing and Materials, West Conshohocken, Pennsylvania.